© 2018. Published by The Company of Biologists Ltd | Journal of Experimental Biology (2018) 221, jeb168625. doi:10.1242/jeb.168625

RESEARCH ARTICLE

Femoral bone perfusion through the nutrient foramen during growth and locomotor development of western grey kangaroos (*Macropus fuliginosus*)

Qiaohui Hu[1], Thomas J. Nelson[1], Edward P. Snelling[2] and Roger S. Seymour[1,*]

ABSTRACT

The nutrient artery passes through the nutrient foramen on the shaft of the femur and supplies more than half of the total blood flow to the bone. Assuming that the size of the nutrient foramen correlates with the size of the nutrient artery, an index of blood flow rate (Q_i) can be calculated from nutrient foramen dimensions. Interspecific Q_i is proportional to locomotor activity levels in adult mammals, birds and reptiles. However, no studies have yet estimated intraspecific Q_i to test for the effects of growth and locomotor development on bone blood flow requirements. In this study, we used micro-CT and medical CT scanning to measure femoral dimensions and foramen radius to calculate femoral Q_i during the in-pouch and post-pouch life stages of western grey kangaroos (*Macropus fuliginosus*) weighing 5.7 g to 70.5 kg and representing a 12,350-fold range in body mass. A biphasic scaling relationship between Q_i and body mass was observed (breakpoint at ca. 1–5 kg body mass right before permanent pouch exit), with a steep exponent of 0.96±0.09 (95% CI) during the in-pouch life stage and a statistically independent exponent of –0.59±0.90 during the post-pouch life stage. In-pouch joeys showed Q_i values that were 50–100 times higher than those of adult diprotodont marsupials of the same body mass, but gradually converged with them as post-pouch adults. Bone modelling during growth appears to be the main determinant of femoral bone blood flow during in-pouch development, whereas bone remodelling for micro-fracture repair due to locomotion gradually becomes the main determinant when kangaroos leave the pouch and become more active.

KEY WORDS: Allometry, Blood flow, CT scan, Femur, Locomotion, Ontogeny

INTRODUCTION

Long bones are supplied by nutrient, periosteal and epiphyseal blood vessels (Trueta, 1963). In the femur, usually a single nutrient artery enters the bone cortex via the nutrient foramina on the shaft to support more than half of the total blood flow to the femoral bone (Brookes and Revell, 1998; Trueta, 1963). Local blood flow is determined by the oxygen demand of the supplied tissue (Ross et al., 1962; Wolff, 2007). Therefore, femoral bone perfusion is determined by the oxygen requirements of the femoral bone tissue. Femora experience micro-fractures due to stress loading (viz. tension, compression and shearing stresses). An increase in the frequency and magnitude of stress loading during locomotion increases the incidence of micro-fractures, resulting in an increase in bone remodelling (Eriksen, 2010), which is supported by an increase in blood supply (Robling et al., 2006; Lieberman et al., 2003). During bone remodelling, bone matrices are dissolved by osteoclasts and then renewed by osteoblasts associated with capillary loops in the secondary osteons of Haversian bone (Rucci, 2008). An index of blood flow rate (Q_i), based on the size of the femoral nutrient foramina of adult mammals, reptiles and birds, appears to be proportional to locomotor activity levels and can be used as an indicator of general locomotion intensity in living and extinct species (Seymour et al., 2012; Allan et al., 2014).

Although it has been suggested that the rate of blood flow through the femoral nutrient artery corresponds with the locomotor activity levels of terrestrial vertebrates, previous femoral bone blood flow studies using Q_i have considered only the adults of several species (Seymour et al., 2012; Allan et al., 2014). There have been no studies of femoral bone blood flow rate across ontogeny. In addition to repairing micro-fractures, the nutrient artery also supports bone formation (i.e. osteogenesis, bone modelling) during early life stages (Gilbert, 1994). Femoral bone development is classified as endochondral ossification, which refers to early-life skeletal bone formation. The nutrient artery supplies the whole femur shaft, comprising compact bone and trabecular bone below epiphyseal plates, during development (Trueta, 1963). Therefore, femoral bone perfusion and thus the size of the nutrient artery and associated foramen may respond to bone development and growth rate during ontogeny.

This study uses the dimensions of the nutrient foramen as an index of femoral bone blood flow rate and examines its relationship with femoral growth rate and locomotor activity levels during the development of western grey kangaroos, *Macropus fuliginosus*. Newborn marsupial mammals are highly altricial compared with placental mammals, and most developmental processes occur as a joey during the in-pouch stage (Deane and Cooper, 1988). Therefore, kangaroos are ideal subjects to study early lifestage femoral bone blood flow. The limb bones of joeys receive little locomotion stress in the pouch, but the stresses increase as the kangaroo grows, vacates the pouch and becomes independently mobile. We hypothesized that femoral bone perfusion during the in-pouch life stage may correspond with the femoral bone formation rate and growth rate of the animal, and that femoral bone perfusion during the post-pouch life stage is driven primarily by locomotion stresses.

[1]Department of Ecology and Environmental Science, School of Biological Sciences, University of Adelaide, Adelaide, SA 5005, Australia. [2]Brain Function Research Group, School of Physiology, University of the Witwatersrand, Johannesburg, Gauteng 2193, South Africa.

*Author for correspondence (roger.seymour@adelaide.edu.au)

Q.H., 0000-0003-3163-7859; E.P.S., 0000-0002-8985-8737; R.S.S., 0000-0002-3395-0059

Received 20 August 2017; Accepted 14 December 2017

Journal of Experimental Biology (2018) 221, jeb168625. doi:10.1242/jeb.168625

List of abbreviations

L_F	femur length (mm)
L_S	femur shaft length (mm)
M_b	body mass (g)
Q_i	blood flow rate index (mm^3)
R	radius (mm)
V_F	femur volume (cm^3)

MATERIALS AND METHODS

Femur preparation

Carcasses of western grey kangaroos (*Macropus fuliginosus* Desmarest 1817) were obtained from approved culls of the animal in south-eastern South Australia. All culls followed the Code of Practice for the Humane Shooting of Kangaroos (www.environment.gov.au). Individuals were classified as in-pouch or post-pouch by observing their natural behaviour prior to culling and referring to published estimates of the pouch exit body mass (the period between the initial and permanent pouch exit occurs at ca. 2–5 kg) (Poole et al., 1982; Dawson, 2012). In total, 23 pairs of femora were dissected from carcasses weighing 5.7 g to 70.5 kg, representing a 12,350-fold range in body mass. The body mass (M_b, g) of each kangaroo was measured prior to dissection with calibrated scales appropriate for body size. Post-pouch kangaroo femora were cleaned by removing tissue and fur manually and then by warm water maceration for 3 months. Toothbrushes and toothpicks were used to further clean the femora. Unfused epiphyses and segments were re-attached by applying an acetone–acrylic resin adhesive. In-pouch kangaroo femora were not fully calcified and were too fragile to be treated this way. Therefore, in-pouch legs were immersed intact in a 4% formaldehyde fixative solution for 2 weeks and then transferred into a phosphate buffer solution in preparation for micro-CT scanning.

Micro-CT and medical CT scanning

All 23 pairs of femur samples were scanned using a micro-CT scanner (SkyScan-1076; SkyScan-Buker, Kontich, Belgium). Among them, 15 pairs of femora with a maximum length <16 cm were scanned completely (i.e. the complete bone was scanned). For the remaining eight pairs of femora with a maximum length >16 cm, only the small section of the femoral shaft where the foramen was located was scanned. The two largest femur pairs were too large for the scanning bed; therefore, the foramen sections of these four samples had to be excised from the bone shaft using a diamond saw prior to micro-CT scanning. The scanning parameters of the micro-CT scanner were adjusted to account for variation in femoral size. Pixel size was always less than 11% of foramen radius in a micro-CT image. The raw topographic projection CT image data (TIFF files) were reconstructed using dedicated software (NRecon 1.6.10.4; Bruker microCT, Kontich, Belgium). Reconstruction settings were optimized for each femur to maximize image contrast.

The eight largest femur pairs were not scanned completely using the micro-CT scanner, and therefore they were scanned whole using a larger medical CT scanner (Ingenuity Core 128; Philips, Amsterdam, The Netherlands) in order to obtain femur morphology, including length and volume data. Reconstruction was performed automatically by the scanner's bundled software. The raw CT image data (DICOM files) were converted into useable raster image files (BMP files) using the open source image processing software Fiji (www.fiji.sc) and then corrected from anisometric-voxel CT images to isometric-voxel CT images using Fiji and DataViewer 1.5.2.4 (Bruker microCT).

Femur volume and length measurements

Hand-traced regions of interest (ROI) in CT Analyser 1.16.4.1 (Bruker microCT) were used to include regions of the whole bone scanned from both CT scanners. After drawing and saving the ROIs, bone volume images (8-bit, grey scale) were converted to 1-bit binary images using thresholding tools in CT Analyser. The 3D analysis tool was then used to measure femur bone volume (V_F, cm^3) which included the compact bone, trabeculae and bone cavity.

Femora, which were scanned completely using either the micro-CT or medical CT scanner, were realigned vertically in DataViewer, with femur proximal ends pointing downwards. The slice numbers of the upper and lower limits of the whole femur were recorded in CT Analyser. The whole femur length (L_F, mm) was calculated as the product of the number of cross-sectional slices of a sample and the actual pixel size of the image (i.e. thickness of one slice). Femur shaft length (L_S, mm) was also calculated from the upper and lower limits of the femur shaft.

Foramen radius measurements

For each femur, a series of foramen cross-sectional images was obtained using a volume of interest (VOI) tool in DataViewer. The VOIs were traced to include only the regions of the foramina. As VOIs are cuboid shaped, more than one VOI was drawn to account for the curved geometry of the foramen passage in some specimens (Fig. 1). The smallest cross-sectional area of each foramen was measured using Fiji. Foramen radius (R, mm) was then calculated from the area, assuming a perfect circle. Most femora in this study had only one foramen on the bone shaft, except for two specimens which had two foramina. The nominal foramen radius of these femora was calculated from the combined area of the two foramina.

Blood flow rate index calculation

Relative blood flow rate through a bone can be estimated by measuring the size of the foramen that transmits the vessel supplying blood to the bone (Seymour et al., 2012). The method is based on the Poiseuille–Hagen equation ($\dot{Q} = \pi P r^4/8\eta l$), where $\dot{Q}$ is the blood flow rate ($mm^3\ s^{-1}$), P is the pressure difference between two points of a vessel (Pa), r is the vessel lumen radius (mm), η is the blood viscosity (Pa s) and l is the vessel length (mm) between the two points (Pfitzner, 1976). Assuming that foramen size is proportional to the artery size, the Poiseuille–Hagen equation can be simplified to a blood flow rate index (Q_i) relationship, $Q_i = R^4/L$, where Q_i (mm^3) is proportional to blood flow rate, R is the foramen radius (mm) and L is an arbitrary length (mm) related to bone size (in this case, the length of the femur). The equation assumes that blood pressure drop and blood viscosity are constants because they are independent of mammalian body mass except for very large species (Langille, 1996; White and Seymour, 2014). Although

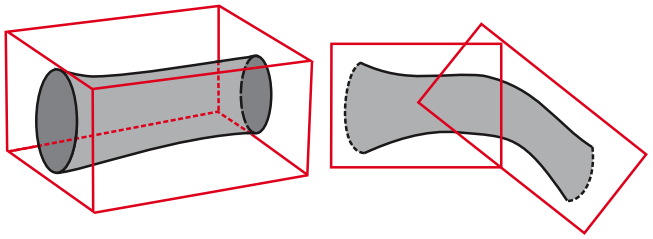

Fig. 1. Schematic diagrams of hand-traced foramen volume of interest (VOI). The diagram on the left is a 3D representation where the red cuboid is the VOI and the grey tube is the foramen passage. The diagram on the right is a 2D representation of the side view of a curved foramen passage with two VOIs.

Journal of Experimental Biology (2018) 221, jeb168625. doi:10.1242/jeb.168625

blood viscosity and blood pressure may change slightly across development, their impact on the blood flow rate index equation is probably negligible in comparison to the effect of R raised to the fourth power. Previous femoral bone blood flow studies have used femur length (L_F) to calculate Q_i (Seymour et al., 2012; Allan et al., 2014). However, L_F of western grey kangaroos in this study was difficult to quantify accurately because some femur samples had incompletely developed epiphyses. Femur shaft length (L_S), which is the distance between the epiphyses, is a relatively precise substitution but it cannot be used for comparing Q_i with the femoral bone blood flow rate index values collected in previous studies that used total length. Therefore, to allow for comparison between individuals in the present study with earlier femoral bone blood flow studies, the percentage of epiphysis length of femora with completely developed epiphyses was calculated from the L_F and L_S datasets and then added to the shaft length of femora with no, or incompletely developed, epiphyses.

Statistical analyses

All Q_i and bone morphology data (L_F, L_S, V_F and R) were averaged over both left and right femora of each individual and treated as one datum. Graphs with double log axes were used to present the relationships between Q_i, V_F and M_b; 95% confidence intervals were plotted on the graphs using statistical software (Prism 6.0; GraphPad Software, La Jolla, CA, USA). Broken-stick analysis was used to identify potential breakpoints (i.e. inflection points) in the datasets, indicating a biphasic scaling relationship. The analysis works by fitting a series of two-phase linear regressions to the $\log_{10}$-transformed data and then identifying the point at which the sum of the regressions' residual sums of squares is minimized (Yeager and Ultsch, 1989; Mueller and Seymour, 2011). Although the procedure produced a discrete point, we observed that the shift in slope was gradual. Therefore, we estimated a range of body masses over which the changes occurred. ANCOVA was used to test whether the breakpoint between two phases was statistically significant (Zar, 1998). If ANCOVA indicated that two datasets had significantly different slopes, the Johnson–Neyman test (White, 2003) was used to determine the ranges over which the data were significantly different between the two datasets. All means were reported with 95% confidence intervals.

RESULTS

Biphasic scaling of V_F with M_b

V_F scaled with M_b with a biphasic relationship across development in the western grey kangaroo (Fig. 2). V_F scaled with a steeper exponent of 1.48±0.05 during the in-pouch life stage before transitioning to a significantly shallower exponent of 0.85±0.05 during the post-pouch life stage ($F_{1,19}$=129, P<0.001). The breakpoint occurred at 1–5 kg according to the broken-stick analysis. This corresponds approximately with permanent pouch exit in this species (ca. 5 kg body mass) (Poole et al., 1982; Dawson, 2012).

Biphasic scaling of Q_i with M_b

A biphasic relationship between Q_i and M_b also occurred across development (Fig. 3). Q_i scaled with M_b with a steeper exponent of 0.96±0.09 in the in-pouch joeys compared with a statistically independent exponent of −0.59±0.90 in the post-pouch kangaroos (ANCOVA $F_{1,19}$=29.75, P<0.001). A breakpoint occurred at ca. 1–5 kg body mass. The variability in the post-pouch stage was higher than that in the in-pouch stage, possibly in relation to sex differences. Although the scaling of post-pouch Q_i with M_b was not

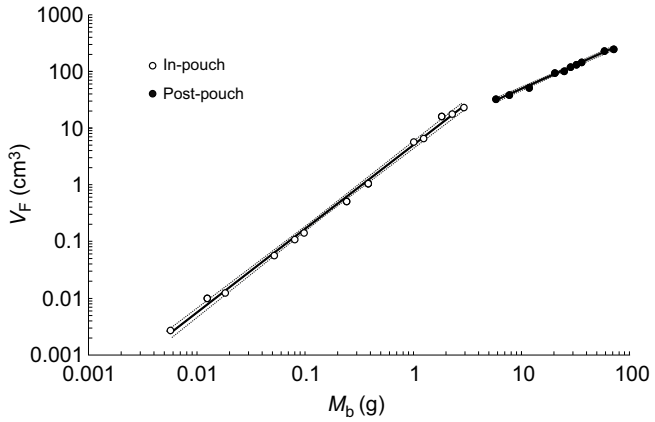

Fig. 2. Scaling of femur volume (V_F) with body mass (M_b) across development in western grey kangaroos. The equation for the in-pouch data is $V_F=1.9\times10^{-4}M_b^{1.48\pm0.05}$ and that for the post-pouch data is $V_F=2.0\times10^{-2}M_b^{0.85\pm0.05}$. The dotted lines represent 95% confidence intervals for each regression mean. The breakpoint occurs at 1–5 kg according to the broken-stick analysis.

significantly different between sexes for comparisons of slope ($F_{1,6}$=0.22, P=0.66) and elevation ($F_{1,7}$=2.15, P=0.19), the average post-pouch male Q_i was approximately 50% greater than the average post-pouch female Q_i.

Biphasic scaling of Q_i with V_F

Scaling of Q_i with V_F also had an initial steep positive exponent of 0.65±0.06 during the in-pouch stage before transitioning to a statistically independent exponent of −0.64±1.08 during the post-pouch stage ($F_{1,19}$=15.34, P<0.001) (Fig. 4). Breakpoint analysis indicated that, as above, a breakpoint occurred at a body mass of 1–5 kg.

DISCUSSION

Biphasic scaling of V_F and Q_i with M_b

The western grey kangaroos analysed in this study had a 12,350-fold body mass range, covering almost the entire lifespan of the species. The scaling of V_F with M_b (Fig. 2) and the scaling of Q_i with M_b

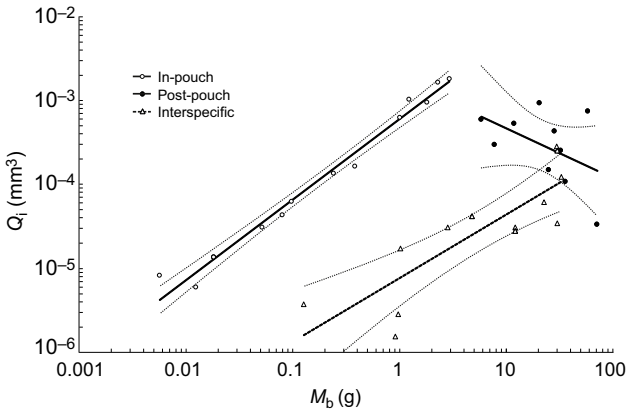

Fig. 3. Scaling of femoral bone blood flow rate index (Q_i) with M_b across development in western grey kangaroos. The equation for the in-pouch data is $Q_i=7.9\times10^{-7}\ M_b^{0.96\pm0.09}$ and that for the post-pouch data is $Q_i=0.11\ M_b^{-0.59\pm0.90}$. The dotted lines represent 95% confidence intervals for each regression mean. The breakpoint occurs at 1–5 kg according to the broken-stick analysis. The dashed line represents interspecific scaling of Q_i across different species of diprotodonts ($Q_i=4.1\times10^{-8}M_b^{0.76\pm0.32}$).

Journal of Experimental Biology (2018) 221, jeb168625. doi:10.1242/jeb.168625

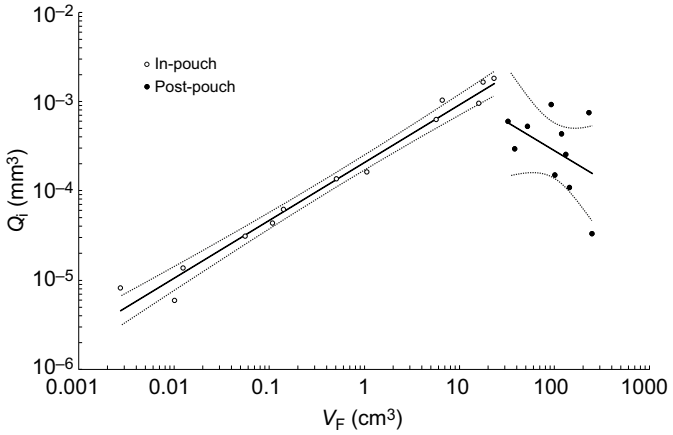

Fig. 4. Scaling of Q_i with V_F across development in western grey kangaroos. The equation for the in-pouch data is $Q_i=2.1\times10^{-4}\ V_F^{\ 0.65\pm0.06}$ and that for the post-pouch data is $Q_i=5.5\times10^{-3}V_F^{\ -0.64\pm1.08}$. The dotted lines represent 95% confidence intervals for each regression mean. The breakpoint occurs at 1–5 kg according to the broken-stick analysis.

(Fig. 3) both showed a significantly higher exponent during the in-pouch life stage than during the post-pouch life stage, with a breakpoint occurring at 1–5 kg, which corresponds approximately with the period during which the joey makes the transition from the in-pouch to the post-pouch life stage (Poole et al., 1982; Dawson, 2012). Biphasic scaling has been observed in cardiac development studies on western grey kangaroos, where relatively steep exponents for heart mass, cardiomyocyte myofibril and mitochondrial volume densities occurred across in-pouch development, and significantly shallower exponents occurred for these parameters during post-pouch development (Snelling et al., 2015a,b). Here, the breakpoint occurred at an M_b of 5–6 kg. The earlier breakpoint for V_F compared with heart mass may be biologically meaningful if development of the femur corresponds with the initial stress loads imposed upon it at initial pouch exit, whereas heart development corresponds with the metabolic perfusion requirements to achieve locomotor independence at permanent pouch exit. Newborn marsupials are ectothermic and maturity of thermoregulation occurs as pouch exit is approached (Rose et al., 1998; Frappell, 2008). Transitioning from ectothermy to endothermy has been suggested to relate to the biphasic scaling of cardiac development in western grey kangaroos (Snelling et al., 2015a). The similar biphasic scaling for Q_i and cardiac development, and the pouch exit breakpoints observed across these relationships, is consistent with the physiological and lifestyle changes that occur at pouch exit as young kangaroos develop endothermy and become independently mobile.

Similar breakpoints for cardiac growth also occur around the time of birth in some placental mammals (Hirokawa, 1972; Mitchell and Skinner, 2009). This transition is critical, and a number of profound anatomical and physiological changes occur. For instance, a sudden rise in the metabolic rate at birth has been observed in goats (Barcroft et al., 1934), sheep (Dawes and Mott, 1959) and rats (Kleiber et al., 1943). Placental mammals can produce a significant amount of heat shortly after birth to adapt to ambient temperature (Asakura, 2004). However, it remains to be investigated whether femoral bone blood flow shows a similar biphasic scaling pattern in placental mammals as we have found for the marsupial kangaroo. We hypothesize that the breakpoint for femoral Q_i occurs around the time of birth in placental mammals.

Comparison of intraspecific and interspecific scaling of Q_i with M_b

Previous interspecific studies on the dimensions of the nutrient foramen have measured its size either directly using calipers or from photomicrographs (Seymour et al., 2012; Allan et al., 2014). However, this study involved micro-CT scanning for all specimens. To compare method differences, all post-pouch nutrient foramen dimensions were also measured from photomicrographs. There are slight, but insignificant, differences in the nutrient foramen size obtained using the different methods. Therefore, intraspecific micro-CT Q_i calculations made in this study can be compared with interspecific photographic Q_i for other mammals. Thirteen diprotodont marsupial species were selected from our previous study (Table S1; Seymour et al., 2012) for comparison with the present data (Fig. 3). Q_i during the in-pouch stage of the western grey kangaroo is approximately 50–100 times higher than the interspecific Q_i of marsupials with a body mass of 0.13–2.9 kg. The significant difference between intraspecific and interspecific Q_i is probably explained by the higher growth rate and hence higher energy and blood flow requirements during development. In many studies, the metabolic rate of growing animals is higher than that of adults with similar body mass (Brody, 1945; Lavigne et al., 1986; Jørgensen, 1988). Mass-specific digestible energy intake of red kangaroo young-at-foot is approximately 1.5 times higher than that of adults; however, energy requirements only for maintaining physiological function are similar in the young and adults (Munn and Dawson, 2003), suggesting that the higher energy intake for the young is used for growth. In addition, relative blood flow through long bones is higher in younger mammals than in older ones (Pasternak et al., 1966; Whiteside et al., 1977; Nakano et al., 1986), suggesting a higher oxygen requirement of long bones during development. A higher oxygen demand may lead to increased nutrient artery size, foramen size and femoral bone blood flow rate. Differences in haemodynamics between developing and adult mammals may also contribute to a larger nutrient foramen during the in-pouch life stage of the kangaroo. For instance, haematocrit (red blood cell density) is lower in juvenile than in adult mammals, as has been shown for humans (Gonez et al., 1993), mice (Jones et al., 2004), fur seals and sea lions (Horning and Trillmich, 1997; Fowler et al., 2007). In addition, although blood pressure is independent of adult body mass across smaller species of mammals (White and Seymour, 2014), it may be lower in growing fetuses than in adults, as has been shown in humans (Struijk et al., 2008) and suggested in western grey kangaroos (Snelling et al., 2015a). Therefore, in-pouch kangaroos may have lower blood oxygen content and blood pressure, and so may require relatively larger arteries for blood perfusion. Vessel wall thickness may be another determinant of foramen size as, upon dissection, aortas of early in-pouch kangaroos were observed to have relatively thicker walls than those of later in-pouch and post-pouch kangaroos (Q.H., T.J.N., E.P.S. and R.S.S., unpublished observations). However, as the aortas were not observed under the physiological strain of blood pressure, the veracity of this observation remains uncertain. Differences in blood flow regime may also require a larger foramen on in-pouch femora. In younger femora, there is no periosteal blood supply to the bone cortex; however, periosteal blood supply becomes more important with age after maturity (Bridgeman and Brookes, 1996). Even after considering all possible factors, it is difficult to explain the significant difference between the intraspecific and interspecific Q_i. Thus, future studies on the relationship between vessel size and foramen size are necessary. Unsurprisingly, the intraspecific scaling of Q_i in post-pouch

Journal of Experimental Biology (2018) 221, jeb168625. doi:10.1242/jeb.168625

kangaroos tends to merge with the interspecific line (Fig. 3). A Johnson–Neyman test indicates that post-pouch kangaroos with body masses greater than 28 kg have Q_i that are statistically indistinguishable from the interspecific Q_i.

Determinants of Q_i during in-pouch and post-pouch life stages

Kangaroo femoral Q_i scales with body mass with an exponent of 0.96±0.09 during the in-pouch life stage, and then becomes independent of body mass during the post-pouch life stage, scaling with an exponent of –0.59±0.90 (Fig. 3). The factors driving femoral Q_i during the in-pouch and post-pouch life stages are probably different. Local tissue metabolic rate determines local blood flow rate (Ross et al., 1962). The oxygen demand of tissues such as the brain, heart and skeletal muscle determines a proportionate blood supply (Wolff, 2007). An exception is the kidney, in which renal plasma flow determines metabolic rate (Valtin, 1973). Although the situation for bone is unknown, we believe that the oxygen demand of bone tissue determines the blood flow rate because increasing loading or exercise leads to increased energy-dependent bone remodelling and bone perfusion (Lieberman et al., 2003; Robling et al., 2006). In addition, when oxygen is not available to bones during growth, osteoblasts detect hypoxia and trigger the hypoxia-inducible factor α pathway to stimulate angiogenesis and osteogenesis (Wang et al., 2007). As nutrient arteries provide more than half of the total blood supply to the long bones (Trueta, 1963), blood flow through the nutrient foramen should correlate with the oxygen demand of the femoral bone tissue. Growth is considered to be the major determinant of Q_i during the in-pouch stage, not only because of the noticeable difference in Q_i between the in-pouch intraspecific and interspecific scaling relationships (Fig. 3) but also because the scaling exponent of the in-pouch Q_i is not significantly different from 1.0. Previous studies have shown that when the cost of growth predominates over the cost of maintenance, the scaling of metabolic rate with body mass tends towards isometry (Wieser, 1994; Jørgensen, 1988). Before leaving the pouch, joeys grow in a stable environment without significant stresses on their limb bones. Therefore, growth can be seen as the predominant factor driving Q_i during the in-pouch life stage.

Like most organisms, kangaroos exhibit a characteristic sigmoidal body growth curve, generally growing slowly at the beginning, then increasing growth rate, and finally decreasing it later in development (Cockburn and Johnson, 1988). Poole et al. (1985) recorded the age and body mass of western grey kangaroos (Table S2, Fig. 5A). We have combined their data with our V_F data (Table S3) to generate a femur growth curve (Fig. 5B). The femur growth curve is also sigmoidal. The body and femur growth rates are the highest at body masses equal to 4.7 and 2.0 kg, respectively, which approximately correspond with the pouch exit body mass when compared with the broad body mass range of the whole lifespan. In addition, the scaling of V_F with M_b indicates a faster femur growth rate during the period between the initial and permanent pouch exit (Fig. 2). Limb bones of kangaroos grow very rapidly before the animal leaves the pouch (Dawson, 2012) because joeys need to develop sufficiently strong femora in the pouch to be able to support their own weight at the first pouch exit.

In contrast to the patterns observed for the scaling of in-pouch Q_i, post-pouch Q_i is not significantly correlated with either body mass or bone volume (Figs 3 and 4). After kangaroos leave the pouch and become independently mobile, their growth rate decreases and locomotor activity level increases. For post-pouch kangaroos, the main determinant of oxygen demand for femoral bone tissue gradually changes from growth to locomotion. Although no studies have investigated the difference in the oxygen demand of a growing bone compared with that of a mature bone, we believe that the oxygen needed for bone remodelling is likely to be less than that needed for growth, because bone mass is considered to be constant during bone remodelling, whereas it increases during development (Rucci, 2008). Future studies are required to provide evidence for the metabolic energy requirements of growing bone. During the in-pouch life stage, the body mass of male and female western grey kangaroos is similar (Poole et al., 1982), whereas males tend to have a higher growth rate than the females after pouch exit (Dawson, 2012). The growth rate difference between sexes may account for some of the great variability of Q_i during the post-pouch life stage.

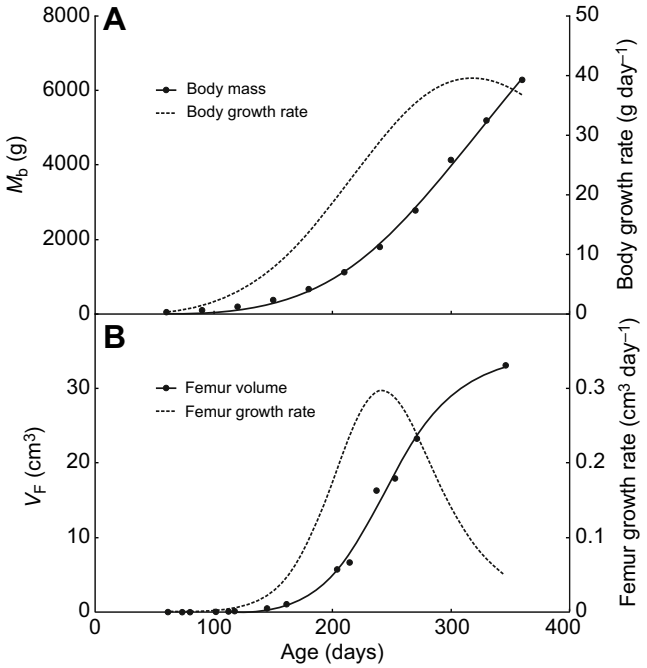

Fig. 5. Relationships between M_b, V_F and age of western grey kangaroos in the first year of development. (A) M_b vs age (A) (solid line) where $M_b=(12{,}067\times A^{4.39})/(352^{4.39}+A^{4.39})$ (average of males and females from Poole et al., 1985); body growth rate vs A (dashed line). (B) V_F vs A (solid line) where $V_F=(35.05\times A^{8.30})/(248.4^{8.30}+A^{8.30})$; femur growth rate vs A (dashed line).

Conclusions

The ontogenetic femoral bone blood flow of western grey kangaroos follows a biphasic scaling pattern, where a breakpoint splitting the two phases occurs at pouch exit. During the in-pouch life stage, a high growth rate appears to be the main factor that determines femoral bone blood flow. After permanent pouch exit, growth rate decreases and the kangaroo becomes independently mobile. Thus, during the post-pouch life stage, micro-fracture repair and remodelling probably become the main factors driving blood flow requirements.

Acknowledgements

We thank David Stemmer and Cath Kemper from the South Australian Museum for allowing access to their facilities. Ruth Williams and Agatha Labrinidis from Adelaide Microscopy and Ben Whigmore and Bill Loftus from Sound Radiology lent their expertise on CT scanners. John Snelling, Marc Jones and David Taggart from the University of Adelaide assisted in the field and in the laboratory. Tomasz Owerkowicz from California State University and one anonymous reviewer provided helpful advice on the manuscript. The authors acknowledge the humane method of the management culls and thank the marksman for allowing access to carcasses.

Competing interests
The authors declare no competing or financial interests.

Author contributions
Conceptualization: Q.H., R.S.S.; Methodology: Q.H., T.J.N., E.P.S., R.S.S.; Validation: Q.H., T.J.N., E.P.S., R.S.S.; Formal analysis: Q.H., E.P.S.; Investigation: Q.H., E.P.S.; Resources: E.P.S., R.S.S.; Data curation: Q.H., T.J.N.; Writing - original draft: Q.H.; Writing - review & editing: Q.H., T.J.N., E.P.S., R.S.S.; Supervision: T.J.N., E.P.S., R.S.S.; Project administration: R.S.S.; Funding acquisition: R.S.S.

Funding
This research was supported by an Australian Research Council Discovery Project Grant [DP-120102081]. E.P.S. holds a South African Claude Leon Foundation Postdoctoral Fellowship.

Data availability
Data are available from ResearchGate: https://www.researchgate.net/profile/Qiaohui_Hu

Supplementary information
Supplementary information available online at
http://jeb.biologists.org/lookup/doi/10.1242/jeb.168625.supplemental

References

Allan, G. H., Cassey, P., Snelling, E. P., Maloney, S. K. and Seymour, R. S. (2014). Blood flow for bone remodelling correlates with locomotion in living and extinct birds. *J. Exp.Biol.* **217**, 2956-2962.
Asakura, H. (2004). Fetal and neonatal thermoregulation. *J. Nippon Med. Sch.* **71**, 360-370.
Barcroft, J., Flexner, L. B. and McClurkin, T. (1934). The output of the foetal heart in the goat. *J. Physiol. London.* **82**, 489-508.
Brody, S. (1945). *Bioenergetics and Growth*. New York, NY, US: Reinhold Publishing Corporation.
Bridgeman, G. and Brookes, M. (1996). Blood supply to the human femoral diaphysis in youth and senescence. *J. Anat.* **188**, 611-621.
Brookes, M. and Revell, W. J. (1998). *Blood Supply of Bone: Scientific Aspects*. London, UK: Springer.
Cockburn, A. and Johnson, C. N. (1988). Patterns of growth. In *The Developing Marsupial: Models for Biomedical Research* (ed. C.H. Tyndale-Biscoe and P.A. Janssens), pp. 28-40. Berlin: Springer Verlag.
Dawes, G. S. and Mott, J. C. (1959). The increase in oxygen consumption in the lamb after birth. *J. Physiol. London.* **146**, 295-315.
Dawson, T. J. (2012). *Kangaroos*. Collingwood, Victoria, Australia: CSIRO Publishing.
Deane, E. and Cooper, D. (1988). Immunological development of pouch young marsupials. In *The Developing Marsupial* (ed. C. Tyndale-Biscoe), pp. 190-199. Berlin: Springer.
Eriksen, E. F. (2010). Cellular mechanisms of bone remodelling. *Rev. Endocr. Metab. Disord.* **11**, 219-227.
Fowler, S. L., Costa, D. P., Arnould, J. P. Y., Gales, N. J. and Burns, J. M. (2007). Ontogeny of oxygen stores and physiological diving capability in Australian sea lions. *Funct. Ecol.* **21**, 922-935.
Frappell, P. B. (2008). Ontogeny and allometry of metabolic rate and ventilation in the marsupial: matching supply and demand from ectothermy to endothermy. *Comp. Biochem. Physiol. A.* **150**, 181-188.
Gilbert, S. F. (1994). Osteogenesis: the development of bones. In *Development Biology* (ed. S. F. Gilbert), pp. 333-338. Sunderland, MA, US: Sinauer Associates.
Gonez, C., Donayre, M., Villena, A. and Gonzales, G. F. (1993). Haematocrit levels in children at sea level and at high altitude: effect of adrenal androgens. *Hum. Biol.* **65**, 49-57.
Hirokawa, K. (1972). A quantitative study on pre- and postnatal growth of human heart. *Acta Pathol. Jpn.* **22**, 613-624.
Horning, M. and Trillmich, F. (1997). Development of hemoglobin, haematocrit, and erythrocyte values in Galapagos fur seals. *Mar. Mamm. Sci.* **13**, 100-113.
Jones, E. A. V., Baron, M. H., Fraser, S. E. and Dickinson, M. E. (2004). Measuring hemodynamic changes during mammalian development. *Am. J. Physiol. Heart Circ. Physiol.* **287**, H1561-H1569.
Jørgensen, C. B. (1988). Metabolic costs of growth and maintenance in the toad, *Bufo bufo*. *J. Exp. Biol.* **138**, 319-331.
Kleiber, M., Cole, H. H. and Smith, A. H. (1943). Metabolic rate of rat fetuses *in vitro*. *J. Cell. Comp. Pathol.* **22**, 167-176.
Langille, B. L. (1996). Arterial remodelling: relation to haemodynamics. *Can. J. Physiol. Pharmacol.* **74**, 834-841.
Lavigne, D. M., Innes, S., Worthy, G. A. J., Kovacs, K. M., Schmitz, O. J. and Hickie, J. P. (1986). Metabolic rates of seals and whales. *Can. J. Zool.* **64**, 279-284.
Lieberman, D. E., Pearson, O. M., Polk, J. D., Demes, B. and Crompton, A. W. (2003). Optimization of bone growth and remodelling in response to loading in tapered mammalian limbs. *J. Exp. Biol.* **206**, 3125-3138.
Mitchell, G. and Skinner, J. D. (2009). An allometric analysis of the giraffe cardiovascular system. *Comp. Biochem. Physiol. A Mol. Integr. Physiol.* **154**, 523-529.
Mueller, C. A. and Seymour, R. S. (2011). The regulation index: a new method for assessing the relationship between oxygen consumption and environmental oxygen. *Physiol. Biochem. Zool.* **84**, 522-532.
Munn, A. J. and Dawson, T. J. (2003). Energy requirements of the red kangaroo (*Macropus rufus*): impacts of age, growth and body size in a large desert-dwelling herbivore. *J. Comp. Physiol. [B]* **173**, 575-582.
Nakano, T., Thompson, J. R., Christopherson, R. J. and Aherne, F. X. (1986). Blood flow distribution in hind limb bones and joint cartilage from young growing pigs. *Can. J. Vet. Res.* **50**, 96-100.
Pasternak, H. S., Kelly, P. J. and Owen, C. A., Jr (1966). Estimation of oxygen consumption, and carbon dioxide production and blood flow of bone in growing and mature dogs. *Mayo Clin. Proc.* **41**, 831-835.
Pfitzner, J. (1976). Poiseuille and his law. *Anaesthesia* **31**, 273-275.
Poole, W. E., Carpenter, S. M. and Wood, J. T. (1982). Growth of grey kangaroos and the reliability of age determination from body measurements II. the western grey kangaroos, *Macropus fuliginosus fuliginosus, M. f. melanops* and *M. f. ocydromus*. *Aust. Wildl. Res.* **9**, 203-212.
Poole, W. E., Carpenter, S. M. and Wood, J. T. (1985). Growth of grey kangaroos and the reliability of age determination from body measurements. II. the western grey kangaroos, *Macropus fuliginosus fuliginosus*, *M. f. melanops* and *M. f. ocydromus*: a correction. *Aust. Wildl. Res.* **12**, 561-562.
Robling, A. G., Castillo, A. B. and Turner, C. H. (2006). Biomechanical and molecular regulation of bone remodelling. *Annu. Rev. Biomed. Eng.* **8**, 455-498.
Rose, R. W., Kuswanti, N. and Colquhoun, E. Q. (1998). Development of endothermy in a Tasmanian marsupial, *Bettongia gaimardi* and its response to cold and noradrenaline. *J. Comp. Physiol. [B]* **168**, 359-363.
Ross, J. M., Guyton, A. C., Fairchild, H. M. and Weldy, J. (1962). Autoregulation of blood flow by oxygen lack. *Am. J. Physiol.* **202**, 21-24.
Rucci, N. (2008). Molecular biology of bone remodelling. *Clin. Cases Miner. Bone. Metab.* **5**, 49-56.
Seymour, R. S., Smith, S. L., White, C. R., Henderson, D. M. and Schwarz-Wings, D. (2012). Blood flow to long bones indicates activity metabolism in mammals, reptiles and dinosaurs. *Proc. R. Soc. B* **279**, 451-456.
Snelling, E. P., Taggart, D. A., Maloney, S. K., Farrell, A. P. and Seymour, R. S. (2015a). Biphasic allometry of cardiac growth in the developing kangaroo *Macropus fuliginosus*. *Physiol. Biochem. Zool.* **88**, 216-225.
Snelling, E. P., Taggart, D. A., Maloney, S. K., Farrell, A. P., Leigh, C. M., Waterhouse, L., Williams, R. and Seymour, R. S. (2015b). Scaling of left ventricle cardiomyocyte ultrastructure across development in the kangaroo *Macropus fuliginosus*. *J. Exp.Biol.* **218**, 1767-1776.
Struijk, P. C., Mathews, V. J., Loupas, T., Stewart, P. A., Clarks, E. B., Steegers, E. A. P. and Wladimiroff, J. W. (2008). Blood pressure estimation in the human fetal descending aorta. *Ultrasound Obstet. Gynecol.* **32**, 673-681.
Trueta, J. (1963). The role of the vessels in osteogenesis. *J. Bone Joint Surg. Br.* **45**, 402-418.
Valtin, H. (1973). *Renal Function: Mechanisms Preserving Fluid and Solute Balance in Health*. Boston, MA, US: Little, Brown.
Wang, Y., Wan, C., Deng, L., Liu, X., Cao, X., Gilbert, S. R., Bouxsein, M. L., Faugere, M.-C., Guldberg, R. E., Gerstenfeld, L. C. et al. (2007). The hypoxia-inducible factor α pathway couples angiogenesis to osteogenesis during skeletal development. *J. Clin. Invest.* **117**, 1616-1626.
White, C. R. (2003). Allometric analysis beyond heterogeneous regression slopes: use of the Johnson-Neyman technique in comparative biology. *Physiol. Biochem. Zool.* **76**, 135-140.
White, C. R. Seymour, R. S. (2014). The role of gravity in the evolution of mammalian blood pressure. *Evolution* **68**, 901-908.
Whiteside, L. A., Simmons, D. J. and Lesker, P. A. (1977). Comparison of regional bone blood flow in areas with differing osteoblastic activity in the rabbit tibia. *Clin. Orthop.* **124**, 267-270.
Wieser, W. (1994). Cost of growth in cells and organisms: general rules and comparative aspects. *Biol. Rev.* **69**, 1-33.
Wolff, C. B. (2007). Normal cardiac output, oxygen delivery and oxygen extraction. *Adv. Exp. Med. Biol.* **599**, 169-182.
Yeager, D. P. and Ultsch, G. R. (1989). Physiological regulation and conformation: a BASIC program for the determination of critical points. *Physiol. Zool.* **62**, 888-907.
Zar, J. H. (1998). *Biostatistical Analysis*. New Jersey: Prentice-Hall, Inc.